J. Fluid Mech. (1979), *vol.* 93, *part* 2, *pp.* 281–303
Printed in Great Britain

Shear fluctuations in a turbulent jet shear layer

By M. R. DAVIS

School of Mechanical and Industrial Engineering,
University of New South Wales, Kensington, Australia

AND P. O. A. L. DAVIES

Institute of Sound and Vibration Research,
University of Southampton, England

(Received 14 March 1978 and in revised form 19 November 1978)

The initial development of turbulence in the shear layer of a circular jet is observed to show disturbances of increasing scale at discrete frequencies in an approximate 4:2:1 sequence. These are completely confined within the laminar shear layer and convect at 0·59 of the jet velocity. Such relatively regular behaviour was not observed once the disturbances became larger in transverse dimension than the laminar shear layer.

In the development of the subsequent turbulent shear layer it was found that the fluctuating turbulent shear did not scale with local mean shear, but rather scaled more closely with the minus half power of distance from the apparent origin of the laminar shear layer emanating from the nozzle. The scale of the shear fluctuations departed from growth in proportion to shear layer thickness, remaining almost constant. In these aspects it appears that the turbulent shear layer is not well described by a similar growth with axial distance.

The shear fluctuations convected at a speed closer to the local mean velocity than do velocity fluctuations and showed a relatively more patchy distribution with a distinct rotational sense and no reversal of skewness across the layer. Velocity fluctuations showed phase lags approaching $\frac{1}{3}\pi$ relative to shear fluctuations suggesting that dominant velocity disturbances are those associated with entrainment behind concentrations of rotation.

1. Introduction

Turbulent shear layers have been found to exhibit strongly intermittent behaviour in many cases whilst more recently evidence of large-scale regular structures has been found. The study of intermittency (e.g. Kovasznay, Kibens & Blackwelder, 1970) requires firstly the establishment of a criterion for distinguishing turbulent and non-turbulent regions of flow. Such criteria have included the magnitude of velocity excursions (Davies, Bruun & Baxter 1975), the magnitude of velocity time derivative excursions (Townsend 1976), or the magnitude of the unsteady vorticity in the flow (Browand & Weidman 1976; Corrsin & Kistler 1955). The problem of measuring the complete vorticity has often led to the use of one of its component terms (e.g. $\partial u/\partial y$) as an indicator of turbulence as in the last references quoted. Where large-scale structures have been examined (as summarized by Davies & Yule, 1975), these have

0022-1120/79/4247-6880 $02.00 © 1979 Cambridge University Press

often been considered in terms of highly convoluted and stretched sheets of concentrated vorticity which arise from the instability of some initial laminar shear layer. It is apparent, therefore, that the detection of vorticity, or at least one of its components, can play an important role in both the detection of turbulent and non-turbulent regions and in examining large-scale structures.

Two relatively simple methods may be conceived by which the use of hot wire probes may be extended to determine component terms of the vorticity. In view of the difficulties in accurately calibrating hot wires for determination of velocity components (Morrison, Perry & Samuel 1972; Davis & Davies 1972) it is evident that a relatively simple method is desirable. This is a particularly relevant aspect, as formation of the differences of instantaneous velocity signals must be involved and these would be subject to greater errors, especially if the anemometers are not accurately matched. Firstly, a pair of closely spaced wires, parallel to each other and normal to the stream mean flow, may be used to indicate the unsteady gradient $(\partial u/\partial y)$, where (u, v, w) are the velocity components in the (x, y, z) directions, the mean flow being along the x direction (Kovasznay *et al.* 1970). Secondly, an array of four wires in the form of an X, each set at 45° to the mean flow and with one wire on each arm of the X, may be used to indicate the vorticity at right angles to the plane of the X by appropriate summation and differencing of the four wire signals (Kistler 1952; Kovasznay 1954). More complex arrangements would increase the size of the sensing array and would considerably complicate the calibration method. Of the two arrangements proposed, it is evident that the former offers the possibility of using a smaller incremental distance over which a velocity difference is measured, as the X array is severely limited by wire length and mounting considerations. It was therefore decided to carry out the present investigations using a simple pair of parallel wires so that small spacings could be adopted if found necessary, and also so that the complications of inclined wire calibrations would be avoided.

2. Initial development in the turbulent shear layer

The experimental work was carried out in the mixing layer of a 5·08 cm diameter circular jet, the flow being essentially identical to that described by Davies, Fisher & Barrett (1963) in the initial region. As a precaution measurements of turbulence intensity and mean velocity were made and found to agree closely with the earlier published data in the zone $x/D \leqslant 6$. Measurements were made with 2 mm long, 5 μm diameter tungsten hot wires, operated in a constant resistance feedback anemometer with a 10 point diode chain linearizer. Calibrations of the system showed the output to be linear to within 1 % over a 75 m/s total range, although variations in the system sensitivity to velocity changes $(\partial E/\partial u)$, E being the output voltage, would be somewhat larger with variations of around 3 % in the range of velocities used. The maximum jet velocity used was 50 m/s so that the rather larger errors in the instrument sensitivity close to the upper limit of its total range of calibration were not encountered.

The initial shear layer from the nozzle was laminar with a thickness determined by the boundary layer formed on the inside wall of the converging nozzle, which had an area contraction ratio of 9 :1 and a contraction length of 0·21 m. The development of initially regular disturbances within the shear layer is shown by the single wire measurements in figure 1, as the shear layer was too thin at this position to allow the

use of parallel wire probe. At the closest position to the nozzle ($x/D = 0{\cdot}025$) the disturbances were found to be very regular indeed, the autocorrelation function showing virtually no bandwidth damping. No artificial stimulation was applied to the jet in making the measurements shown in figure 1, as in the experiments of Crow & Champagne (1971) or Moore (1977) who obtained evidence of regular disturbances at much greater distances. Moore also obtained evidence of regular disturbances without artificial stimulation. The very regular disturbances were only detected fairly close to the centre of the shear layer where the mean local speed lay in the range $0{\cdot}2U_j < U < 0{\cdot}5U_j$ approximately. The Schlieren photographs of Davis (1971) also show these regular disturbances in the initial shear layer quite distinctly over the range $0 < x/D < 0{\cdot}20$, and it appears therefore that they are not induced by the anemometer probe employed in the present investigation. Relatively small displacements in the streamwise direction rapidly increased the bandwidth damping of the autocorrelation although the Strouhal number fD/U_j (f denoting frequency, D the nozzle diameter and U_j the jet velocity) of the disturbances appeared to reduce only slightly from 12·5 in the region $0{\cdot}025 \leqslant x/D \leqslant 0{\cdot}075$. At this last position ($x/D = 0{\cdot}075$) there is evidence of disturbances developing at approximately half the Strouhal number of the initial disturbances, this becoming clear at $x/D = 0{\cdot}1$ where the initial disturbances appear to be absent and a Strouhal number of 7·2 is observed. It was not found possible to observe such low bandwidth damping at any position for these lower Strouhal number disturbances, although they could be detected over a wider portion of the shear layer where $0{\cdot}2 < U/U_j < 0{\cdot}85$ at $x/D = 0{\cdot}10$. The second disturbances were no longer evident beyond $x/D = 0{\cdot}175$, and it may be seen from figure 1 that there is slight evidence of yet a third set of disturbances at $x/D = 0{\cdot}225$ with a Strouhal number of approximately 3·2. At this position velocity fluctuations were apparent across the complete shear layer. The frequency of the observed disturbances is more clearly seen in figure 1 (*b*) which shows the spectra of the hot wire signals obtained by Fourier transformation of the complete correlation data. It is also quite clear that at least two frequencies are present together at $x/D = 0{\cdot}075$, whilst the higher frequency component is very much reduced at $x/D = 0{\cdot}10$. The presence of the third disturbance frequency at $St = 3{\cdot}2$ at $x/D = 0{\cdot}200$ may be seen more easily in the spectrum than in the limited section of the correlation shown in figure 1 (*a*).

The results thus show initial disturbances approximately half in frequency at distinct streamwise positions. The disturbances become progressively less regular in the streamwise direction and develop from a region confined completely within the shear layer until they spread across the entire shear layer. The occurrence of only certain dominant frequencies or Strouhal numbers provides strong evidence for the pairing of vortex elements as the instabilities develop (Winant & Browand 1974), but it is clear that in the region where the disturbances were easily identified as regular they lay entirely within the shear layer. It seems therefore that the process observed should be regarded as one of instability within the shear layer rather than a rolling up of the complete sheet of vorticity. Cross correlation measurements with two sensing wires showed that the disturbances appeared to convect at $0{\cdot}59U_j$, that is very close to the velocity at the geometric centre of the shear layer centred on the nozzle lip.

Mean velocity profiles in a radial direction were also measured in the initial shear layer. This was not easy owing to the small thickness of the layer, but results conforming generally to those expected for a laminar free shear layer (see Berger, 1971,

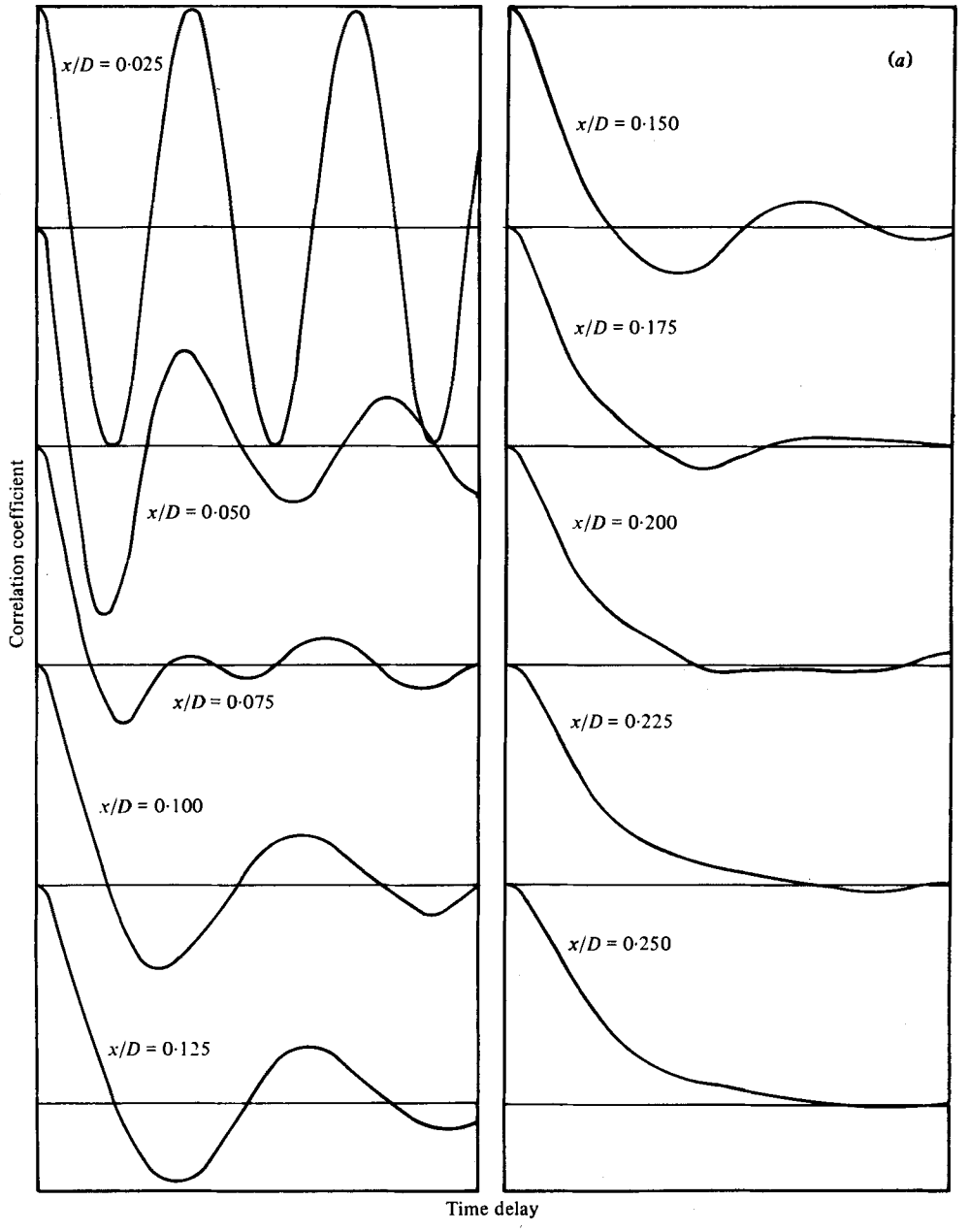

FIGURE 1 (*a*). For legend see facing page.

for example) were found. The variation of maximum shear is shown in figure 2, from which it may be seen that the commencement of the linear growth for the turbulent shear layer corresponds closely in position ($x/D = 0{\cdot}10$) to the point where the observed disturbances in the laminar shear layer had spread almost across the complete shear layer at $St = 7{\cdot}2$. As would be expected the laminar exit shear layer from the nozzle has a higher shear at the higher Reynolds number, and shows a rather earlier

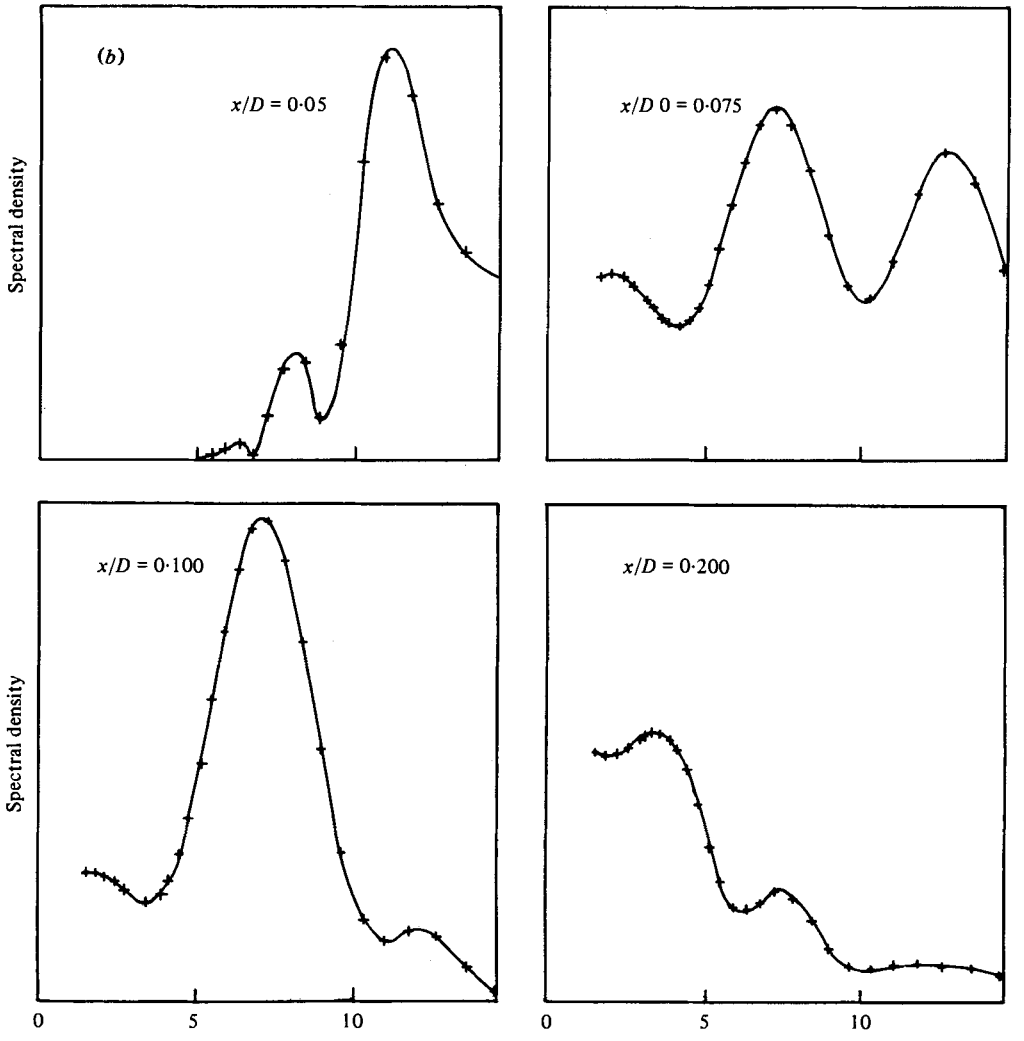

FIGURE 1. (*a*) Autocorrelations of a single hot wire signal in the initial shear layer at $\eta = 0{\cdot}13$ and $Re_\delta = 1{\cdot}16 \times 10^5$. Time delay: 0·333 μs in each case. (*b*) Fourier transforms of correlations in figure 1(*a*). Vertical scale in linear arbitrary units. Horizontal scale: Strouhal number.

approach to the linear shear layer growth relation of the turbulent shear layer. For a restricted axial distance rather higher shear gradients than those of the linearly growing turbulent layer are apparent.

Measurements were also made of the cross correlation of the disturbances in a peripheral direction, and are shown in figure 3. The limited minimum spacing restricts these measurements when the support prongs of the two wires interfere, but it appears that the disturbances have an integral scale in the peripheral sense of approximately 17 mm. This indicates that, although coherence certainly does not exist around the whole shear layer, the disturbances have a dimension in the peripheral direction of the order of 20 times their radial dimension. It might therefore be agreed that they are dominantly two-dimensional in nature. On this basis it is perhaps more representative

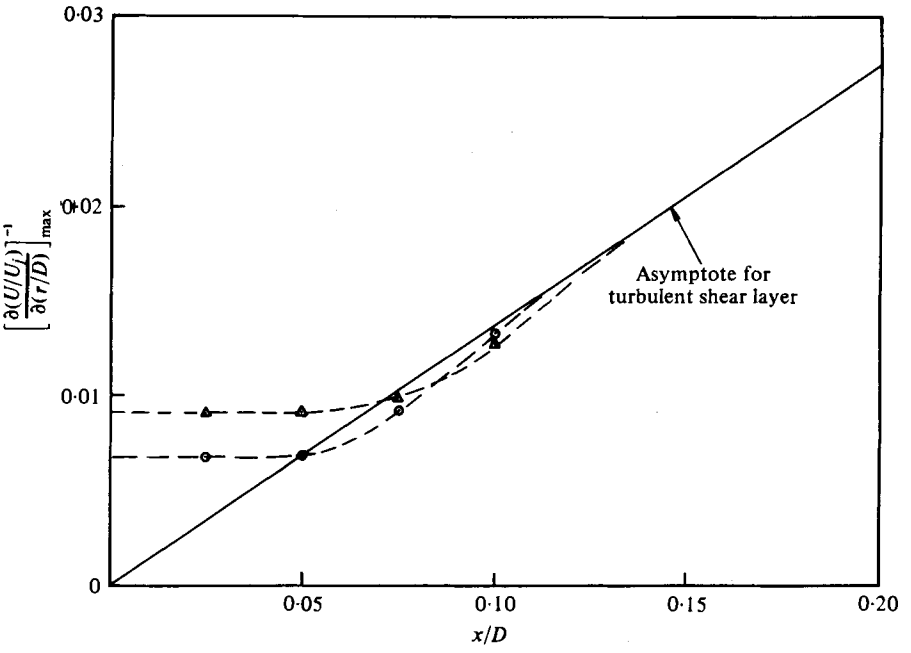

FIGURE 2. Variation of maximum mean shear. △, $Re_j = 0{\cdot}50 \times 10^5$; ⊙, $Re_j = 1{\cdot}16 \times 10^5$. Solid line, asymptote for the turbulent shear layer.

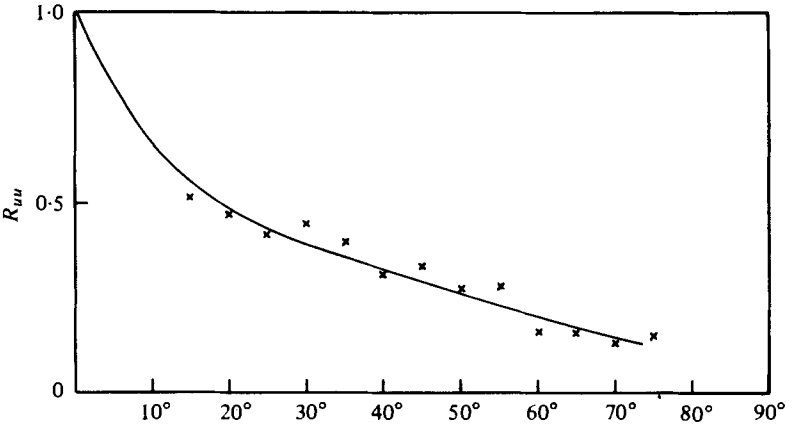

FIGURE 3. Cross correlation of hot wire signals with peripheral displacement. $x/D = 1{\cdot}10$, $\eta = 0$, $Re_j = 1{\cdot}16 \times 10^5$.

to base the observed frequencies on the maximum shear rather than total jet diameter and velocity, giving the three frequencies discussed above as $f(\partial U/\partial y)_{\max} = 0{\cdot}085$, 0·097 and 0·083 at the positions $x/D = 0{\cdot}025$, 0·10 and 0·225 when disturbances are first detected. It is thus apparent that the observed disturbances have wavelengths much longer than their transverse dimension in a radial direction, and that they cannot be physically conceived of in terms of rolling up of a complete vortex sheet as evidenced in many numerical solutions (e.g. Clements & Maull, 1975) where the transverse dimensions of the rolling up sheet are much greater However, it is interesting

to note that the results do show apparently distinct reductions of frequency in a 4:2:1 sequence approximately and although the disturbances must be subject to substantial viscous constraints they lie within the laminar shear layer entirely and have a streamwise wavelength approximately 15 times their dimension in the direction of the shear velocity gradient.

3. Fluctuating shear in the turbulent shear layer

The fluctuating shear $(\partial u/\partial y)'$ was measured using a pair of identical hot wire probes, amplifiers and linearizers. The wires were mounted parallel to each other and at right angles to the flow and to the outward radial vector from the jet axis. It was first necessary to determine a radial spacing between the wires which was small enough that the difference between the two output signals would represent the shear gradient, and yet was kept at a maximum within this requirement so that the signal to noise ratio of the difference signal (obtained from an operational amplifier) representing the shear signal did not deteriorate and more importantly that any spurious components in the shear signal owing to imperfect matching of the 2 channel sensitivities were not magnified. As it was estimated that the system sensitivity $\partial E/\partial U$ could deviate from its ideal value by approximately 3% owing to the influence of slope changes introduced by the break points on the diode chain linearizer, contributions to the shear (velocity difference) signal due to imperfect matching would be at least 15 dB below the level of the velocity fluctuations. However, errors in r.m.s. values will be smaller, perhaps by 3–6 dB depending upon the peak to r.m.s. ratio for the signals, and thus an error of around 18–21 dB below the velocity fluctuations can be achieved. Therefore it is desirable that the wires should not be so closely spaced that the difference signals are lower in level than the velocity signals by values approaching 18 dB if errors due to imperfect matching are to be avoided.

Figure 4 (plate 1) shows typical output signals obtained, and it is immediately apparent that the characteristics of the velocity difference and velocity signals are quite distinct. The velocity difference signal appears dominated by sudden sharp disturbances, interspersed with periods of much smaller fluctuations. As the probe is moved into the shear layer (i.e. a single probe carrying both parallel wires) it appears that increases in shear signal fluctuation intensity occur owing to the greater frequency of the sharp disturbances, rather than due to an increase in their individual magnitude. At the outer edge of the shear layer it may be seen that the sharpest excursions of the shear signal remain in the same sense as on the inner edge, although the signals appear clearer in relation to showing disturbances of dominantly one sense at the inner rather than the outer edge. It appears that these observations are consistent with the sensing probe intercepting a distorted sheet of vorticity, the maximum circulation density in the sheet not varying greatly but the frequency at which the probe intercepts the sheet being greater in the centre of the shear layer.

In order to determine an appropriate spacing between the wires measurements of the magnitude of the velocity difference signal as a function of wire separation were made, as shown in figure 5. It appears that the fluctuations increase in proportion to separation up to a spacing of $\Delta y/D \simeq 0{\cdot}025$ (i.e. $\Delta y = 1{\cdot}3$ mm) beyond which the increase with separation becomes more gradual. It appears that at this separation the shear signal is approximately 0·4 of the velocity signal in magnitude, that is 8 dB

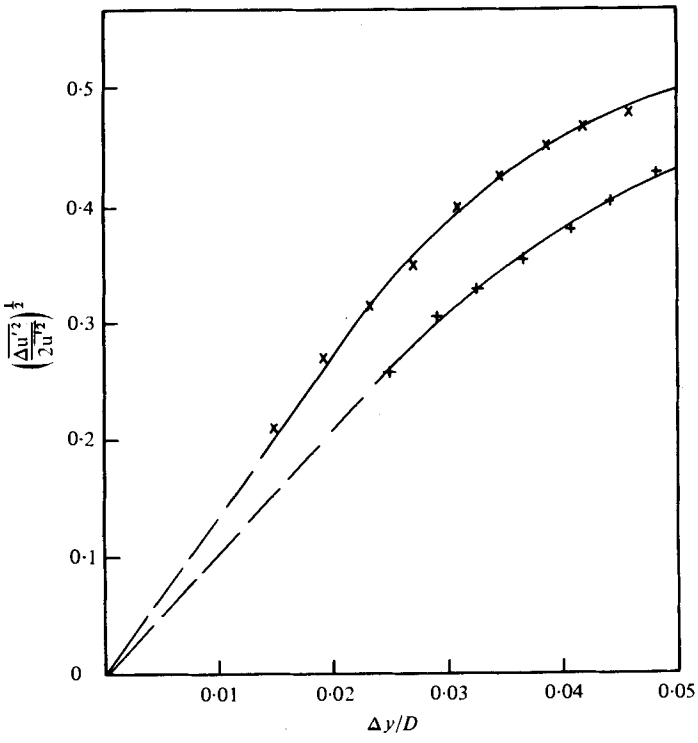

FIGURE 5. Variation of measured velocity difference fluctuations with wire spacing. $Re_\lambda = 1{\cdot}77 \times 10^5$; +, $x/D = 3$; ×, $x/D = 6$; $\eta = 0$.

lower in level. Thus it is expected that the shear signal will contain components due to imperfect matching of the two linearizers which are between 10 and 13 dB smaller than the true velocity difference signal depending upon its peak to r.m.s. ratio. It was felt that a spacing of 1·3 mm thus offered a fair compromise between the introduction of larger errors due to linearizer mis-matching at small separation and the limited spacing over which the difference of velocity at the two wires could be regarded as representing the local shear $(\partial u/\partial y)'$. A probe with a fixed pair of wires with a spacing of 1·34 mm was used in the subsequent measurements. This spacing is appreciably smaller than that used by Kovasznay *et al.* (1970) who also made limited shear measurements with a pair of 2 mm long parallel wires spaced 5 mm apart, although working at lower velocities than those employed here. A very much smaller spacing (0·22 mm) was used by Wygnanski & Fiedler (1970) in examining the turbulent energy balance, but no indication of the precision with which the two anemometers were matched for differencing is given.

The distribution of fluctuating shear within the jet is shown in figure 6. The profiles clearly do not collapse when scaled on the maximum mean shear, which decreases inversely with x/D (see Davies *et al.* 1963). The fluctuating shear reduces by a factor of only 1·5 between $x/D = 1{\cdot}5$ and 6, not by a factor of 4 which would represent the reduction in mean shear over this distance. Thus the unsteady shear does not conform to a simple similarity behaviour related to the mean velocity profile, and an alternative basis for its variation must be sought. On the basis of distance from the nozzle it was

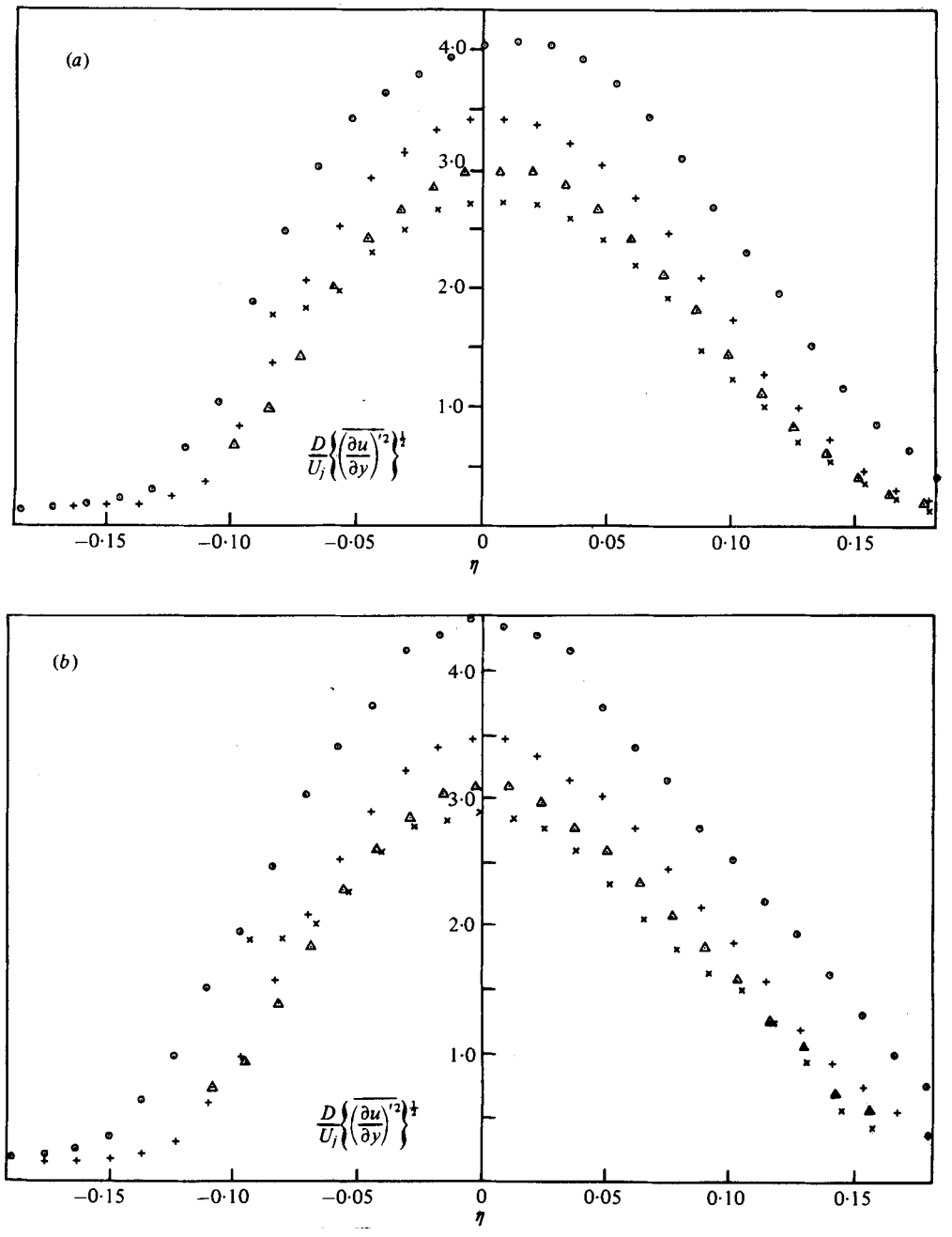

FIGURE 6. Distribution of fluctuating shear (measured with $\Delta y = 0{\cdot}027D$). (*a*) $Re_j = 1{\cdot}77 \times 10^5$. (*b*) $Re_j = 0{\cdot}81 \times 10^5$. ⊙, $x/D = 1{\cdot}5$; +, $x/D = 3{\cdot}0$; △, $x/D = 4{\cdot}5$; ×, $x/D = 6$.

found that the maximum shear fluctuation was a weak function of (x/D), varying with $(x/D)^{-0.29}$ at $Re_j = 1{\cdot}77 \times 10^5$ and with $(x/D)^{-0.34}$ at $Re_j = 0{\cdot}81 \times 10^5$.

These results may be compared with those of Wygnanski & Fiedler (1970) made in a two-dimensional mixing layer. Exact agreement would not be expected as the flow geometries are different and the flow investigated by Wygnanski & Fielder was tripped by a wire at the nozzle lip. The present results conform to the correlation

$$\frac{x}{U_j}\left(\left(\overline{\left(\frac{\partial u}{\partial y}\right)'^2}\right)^{\frac{1}{2}}\right)_{\max} = A\left(\frac{x}{D}\right)^n,$$

where $A = 4{\cdot}63$ and $5{\cdot}08$ and $n = 0{\cdot}71$ and $0{\cdot}66$ at the two jet Reynolds numbers of $1{\cdot}77 \times 10^5$ and $0{\cdot}81 \times 10^5$ respectively. The results of Wygnanski & Fiedler were obtained at a distance of 49·5 cm from the nozzle lip with a velocity of 12 m/s, giving

$$\frac{x}{U_j}\left(\left(\overline{\left(\frac{\partial u}{\partial y}\right)'^2}\right)^{\frac{1}{2}}\right)_{\max} = 35.$$

Applying this last result to the present experiments at an x position which corresponds in Reynolds number based on x for the shear layer, it thus appears that the present experiments yield values which are 43 and 24 % of the values expected from Wygnanski & Fiedler's data applied at $Re_j = 0{\cdot}81 \times 10^5$ and $1{\cdot}77 \times 10^5$ respectively. However, extrapolation of the present data to a lower velocity identical to that of Wygnanski & Fiedler (12 m/s) but at a larger x position than investigated here so that the Re_x values are identical yields a value 25 % below the value obtained by Wygnanski & Fiedler. It thus appears that there is a parameter in addition to Re_x which is influencing the results but that moderate agreement applies at identical velocities and physical distances from the nozzle. It would appear that this velocity effect is in reality an effect due to the nozzle exit flow and its boundary layer which would be related to the nozzle exit Reynolds number Re_j. The rather higher comparative values obtained by Wygnanski & Fiedler (1970) (i.e. by 25 %) could well be caused by a more rapid turbulent development induced by the trip wire.

Comparison may also be made with the self preserving jet results of Wygnanski & Fiedler (1969), although here the geometric differences are greater and an overall scaling on the maximum local velocity (U_m) at a given distance from the nozzle is expected. Wygnanski & Fiedler (1969) give the result

$$\frac{x}{U_m}\left(\left(\overline{\left(\frac{\partial u}{\partial y}\right)'^2}\right)^{\frac{1}{2}}\right)_{\max} = 120$$

for $U_j = 51$ m/s, $x = 185$ cm.

Extrapolation of the present results obtained at $Re_j = 0{\cdot}81$ and $1{\cdot}77 \times 10^5$ respectively to a position with a corresponding Re_x value ($16{\cdot}2 \times 10^5$) gives values which are 75 and 48 % respectively of the measurements of Wygnanski & Fiedler (1969). However, in this case there is, of course, a more substantial difference in flow geometry and close agreement is not expected. However, the present measurements in the initial shear layer of a round jet do thus appear to extrapolate to values comparable with those of Wygnanski & Fiedler (1969).

If the shear layer consists of a structure in which the sheet of vorticity emanating from the nozzle distorts into a complex shape, it might be expected firstly that due

to viscous diffusion the shear gradients will reduce with $(x+x_0)^{-\frac{1}{2}}$, where x_0 is an effective origin which takes account of the finite thickness of the sheet at $x = 0$. Further, increasing complexity of the sheet structure involves stretching of the sheet and a proportionate reduction of its circulation density. Thus it may be argued that the sensing probe signal experiences an increasing number of interceptions of the sheet as its complexity of form increases, but that the magnitude of the shear disturbances sensed at each interception decreases on average and the two effects counteract each other. Thus it may be argued that the measurements of fluctuating shear should reflect only the viscous effect, and vary with $(x+x_0)^{-\frac{1}{2}}$.

The determination of an effective origin for the shear layer emanating from the nozzle may be made on the basis of the behaviour of laminar free shear layers (e.g. Berger, 1971) for which the maximum shear is given at the nozzle exit by

$$\left[\frac{\partial(U/U_j)}{\partial\{y(U_j/\nu x_0)^{\frac{1}{2}}\}}\right]_{\max} = \frac{1}{4{\cdot}7}.$$

Thus, combining this with the measured shear $(\partial(U/U_j)/\partial(y/D))_{\max}$ as shown in figure 2 at the nozzle exit, we find that $x_0 = 2{\cdot}78D$ for $Re_j = 1{\cdot}77 \times 10^5$ and $x_0 = 3{\cdot}29D$ for $Re_j = 0{\cdot}81 \times 10^5$. A regression analysis of the maximum fluctuating shear values shown in figure 6 on this basis shows that if

$$\frac{D}{U_j}\left(\overline{\left(\frac{\partial u}{\partial y}\right)'^2}\right)^{\frac{1}{2}} \sim \left[\frac{x+x_0}{D}\right]^{-n}$$

then $n = 0{\cdot}57$ at $Re_j = 1{\cdot}77 + 10^5$ and $n = 0{\cdot}64$ at $Re_j = 0{\cdot}81 \times 10^5$. Thus it appears that the measured shear fluctuations decrease rather more rapidly with x than would be accounted for simply on the basis of viscous decay. However, the present data certainly lends more support to the argument that the shear layer is composed of a highly distorted sheet of vorticity than to the expectation that the fluctuating shear should scale with the mean shear. The radial distribution of shear fluctuations follows that of the velocity fluctuations closely, reducing to half the maximum at

$$\eta = \left[\frac{y-(D/2)}{x}\right] = 0{\cdot}11.$$

Skewness and flatness factors were measured for both velocity and shear fluctuation from signal amplitude probability distributions and are given in table 1. The reversal of the skewness of the velocity fluctuations discussed by Fisher & Davies (1964) is evident whilst the shear fluctuations show the same skewness on both sides of the shear layer, although appreciably larger values were observed on the inside edge of the shear layer. This is quite consistent with the detection by the probe of strong perturbations of local shear of the same sign as elements of the sheet of vorticity pass over it. The flatness factors for the shear fluctuations were generally much higher than those for velocity fluctuations, reflecting that the vorticity field is comprised of stronger local concentrations. This was particularly evident at the inner edge of the layer where the highest flatness factors were observed. Also it may be noted that the shear fluctuations do not show the same reduction in flatness factor at the centre of the shear layer as do the velocity fluctuations, indicating that the patchiness of the vorticity structure is a more general feature of the turbulent structure. This again is consistent with the

x/D	η	S_u	$S_{(\partial u/\partial y)}$	F_u	$F_{(\partial u/\partial y)}$
1·5	−0·085	−0·10	+1·10	3·01	6·04
	+0·017	+0·06	+0·34	2·45	3·11
	+0·109	+1·07	+0·35	4·04	3·35
3·0	−0·075	−1·04	+1·31	5·27	6·23
	+0·012	+0·07	+0·50	2·48	4·11
	+0·109	+1·10	+0·64	4·14	5·14
4·5	−0·062	−0·96	+0·71	4·11	5·11
	+0·015	+0·08	+0·51	2·45	4·08
	+0·109	+0·82	+0·53	3·20	5·48
6·0	−0·083	−1·06	+0·01	4·28	5·47
	+0·015	+0·23	+0·49	2·84	4·01
	+0·109	+1·00	+0·32	3·76	4·59

TABLE 1. Skewness (S) and flatness (F), factors for velocity (u) and shear ($\partial u/\partial y$) fluctuations.

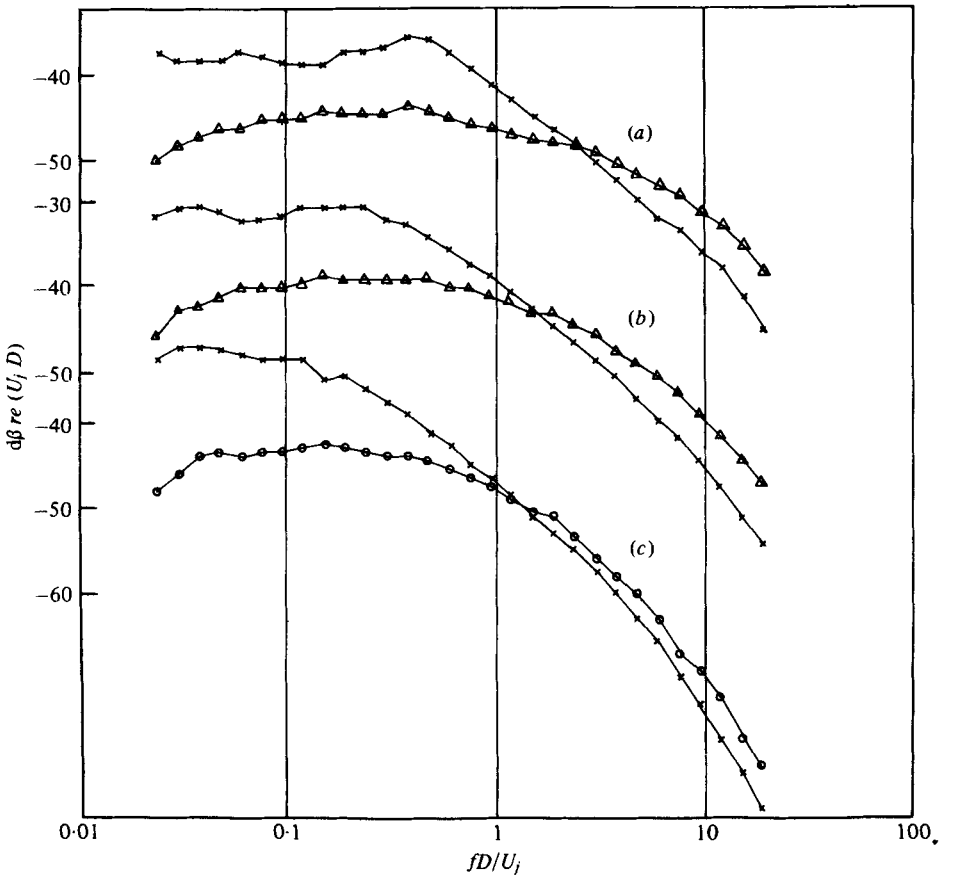

FIGURE 7 (*a*)–(*c*). For legend see facing page.

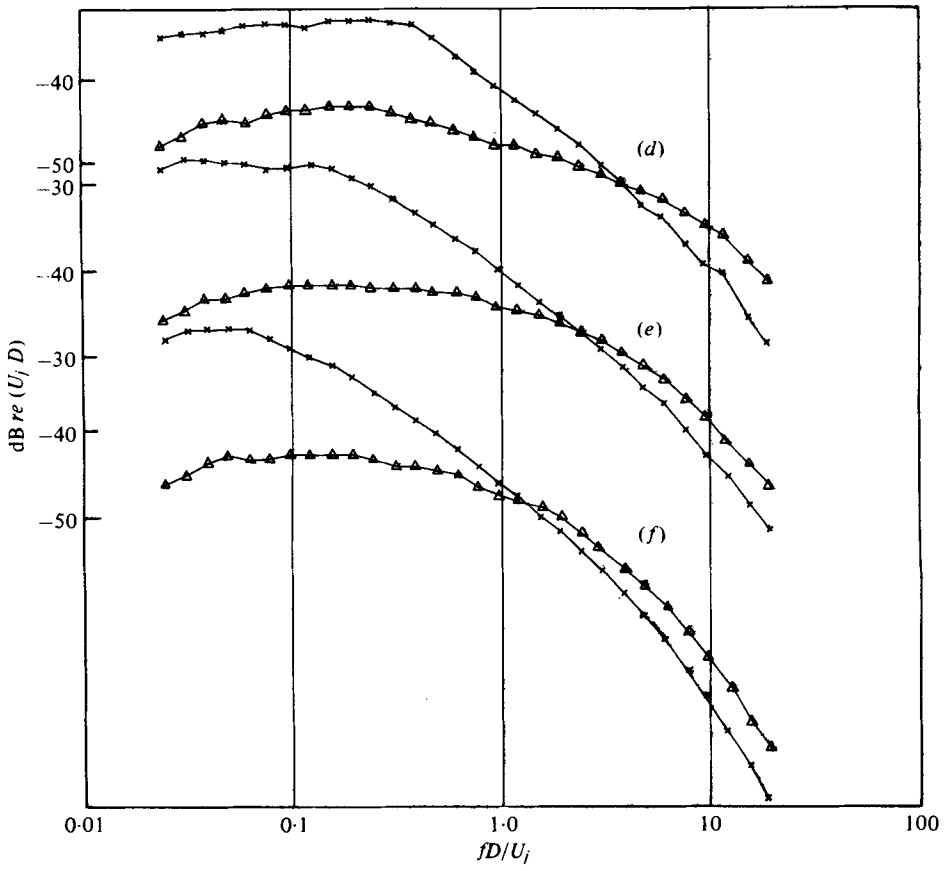

FIGURE 7. Spectra of velocity and velocity difference fluctuations. $Re_j = 1{\cdot}77 \times 10^5$. Spectral density in dB *re* U_jD. ×, velocity spectrum, △, velocity difference spectrum, $\Delta y = 0{\cdot}027D$. (*a*) $x/D = 3$, $\eta = -0{\cdot}067$. (*b*) $x/D = 3$, $\eta = 0{\cdot}013$. (*c*) $x/D = 3$, $\eta = 0{\cdot}100$. (*d*) $x/D = 6$, $\eta = 0{\cdot}167$. (*e*) $x/D = 6$, $\eta = +0{\cdot}006$. (*f*) $x/D = 6$, $\eta = 0{\cdot}165$.

reasoning that the shear layer shows evidence for the presence of a distorted sheet of vorticity.

Comparative frequency spectra of shear and velocity fluctuations measured in third octave bands are shown in figure 7 for some selected positions in the flow. These show that the shear fluctuations contain stronger high frequency components and that the lower frequency components have been reduced by the signal differencing used to provide the shear signal. The relationship between the spectra is shown more clearly in figure 8. It may be noted that the shear spectra do not show a tendency to maintain a constant level above the velocity spectra at high frequency, but rather show an increase relative to the velocity spectra extending to around + 6 dB. This result demonstrates that the high frequency components of the turbulent field are being resolved correctly by the parallel wire sensor, as under conditions where the sensor wire separation was too great there would be a tendency for the wires to show no correlation of components and thus the difference or shear signal would lie 3 dB above the individual velocity signals. This result is not unexpected, as the minimum

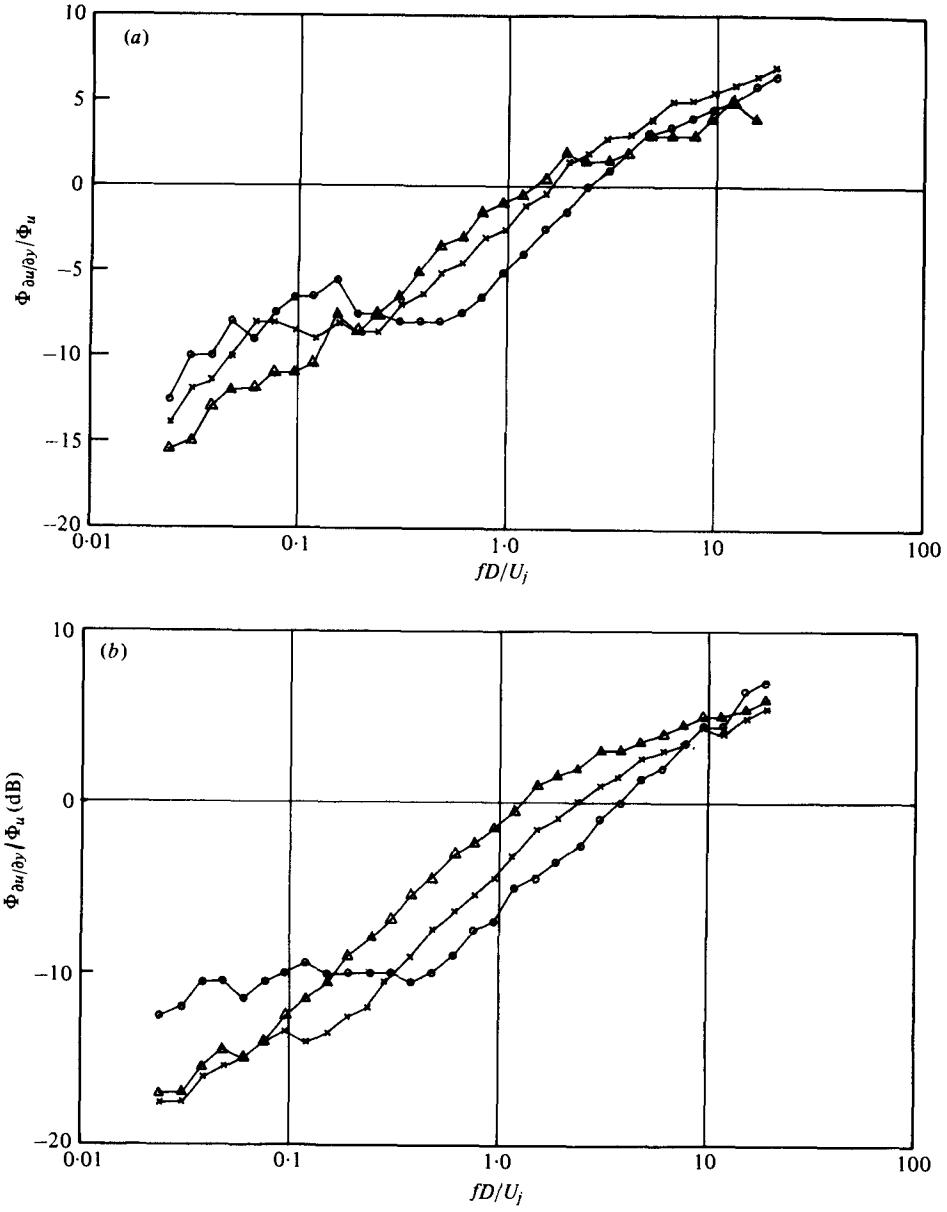

FIGURE 8. Ratio of velocity and velocity difference spectra (from data of figure 7). (*a*) $x/D = 3$: ⊙, $\eta = -0{\cdot}067$; ×, $\eta = 0{\cdot}013$; △, $\eta = 0{\cdot}100$. (*b*) $x/D = 6$: ⊙, $\eta = -0{\cdot}167$; ×, $\eta = 0{\cdot}006$; △, $\eta = 0{\cdot}165$.

Strouhal number shown of around 20 based on jet diameter would become 0·5 if based on the wire separation, indicating that the scale of the smallest fluctuations being resolved is approximately twice the wire separation. It appears that in some cases the results indicate signal inversion of one wire relative to the other, as differences of around + 6 dB arise. However, in view of the 0·5 dB accuracy of the data of figure 7, precise conclusions cannot be made on the basis of these results. However, there is strong support for nearly inverted signal components appearing on each wire at the highest

Re_j	x/D	η	Relative slope (dB/octave)	n
$0{\cdot}81 \times 10^5$	3	−0·045	3·58	1·19
		+0·013	3·38	1·19
		+0·115	3·63	1·20
	6	−0·083	3·77	1·25
		+0·019	3·67	1·22
		+0·098	3·83	1·27
$1{\cdot}77 \times 10^5$	3	−0·067	3·75	1·24
		+0·013	3·25	1·08
		+0·100	3·25	1·08
	6	−0·167	3·46	1·15
		+0·006	3·46	1·15
		+0·165	3·58	1·19

TABLE 2. Relative slopes of velocity and shear spectra.

Strouhal numbers. Data is only presented at frequencies up to approximately one half of the resonant response frequency of the two hot wire amplifier systems, as these were set up with approximately the same damping ratio (0·7, see Davis, 1970) but exact dynamic response matching was not carried out. It may also be seen that at low Strouhal numbers ($fD/U_j \simeq 0{\cdot}1$) the spectra show in all cases components of the shear fluctuations which extend to between 13 and 18 dB lower than the velocity spectra, the results varying somewhat at different positions and to some extent influenced by the lowest frequency (20 Hz) of the analyser used (Bruehl and Kjaer $\frac{1}{3}$ octave filter). This confirms that the previous estimation of the accuracy of the matching of the two linearizers was perhaps slightly conservative as it was made on the basis of the maximum change of sensitivity in the speed range used. Taking account of the likely value of peak to r.m.s. ratio for the signals, it seems that matching to achieve an r.m.s. error 18 dB below the velocity fluctuations is consistent with an estimate of linearizer errors. Certainly these results do not suggest that either wire spacing or linearizer matching was seriously distorting the measurements.

The relative slopes of the shear and velocity spectra which may be noted from figure 8 in the range $0{\cdot}1 < fD/U_j < 5$ approximately (or at rather higher Strouhal numbers on the inner edge where local mean velocities are higher) are shown in table 2. The index n denotes the frequency weighting in the form

$$\Phi_{\partial u/\partial y}(f) \sim f^n \Phi_u(f).$$

The values in table 2 give a mean value for n between the various observations of 1·18. This result thus shows that the turbulent shear layer measurements do not conform to the relation which applies in homogeneous turbulence between the vorticity and velocity spectra, namely

$$\Phi_\omega(k) \sim k^2 \Phi_u(k).$$

The frequency weighting observed is thus appreciably weaker than that to be expected between vorticity and velocity in homogeneous turbulence. However, the flow being studied here is neither homogeneous nor isotropic, and, of course, only one part of component of the vorticity is being measured. It would appear that the very much reduced frequency weighting observed arises from a combination of these effects,

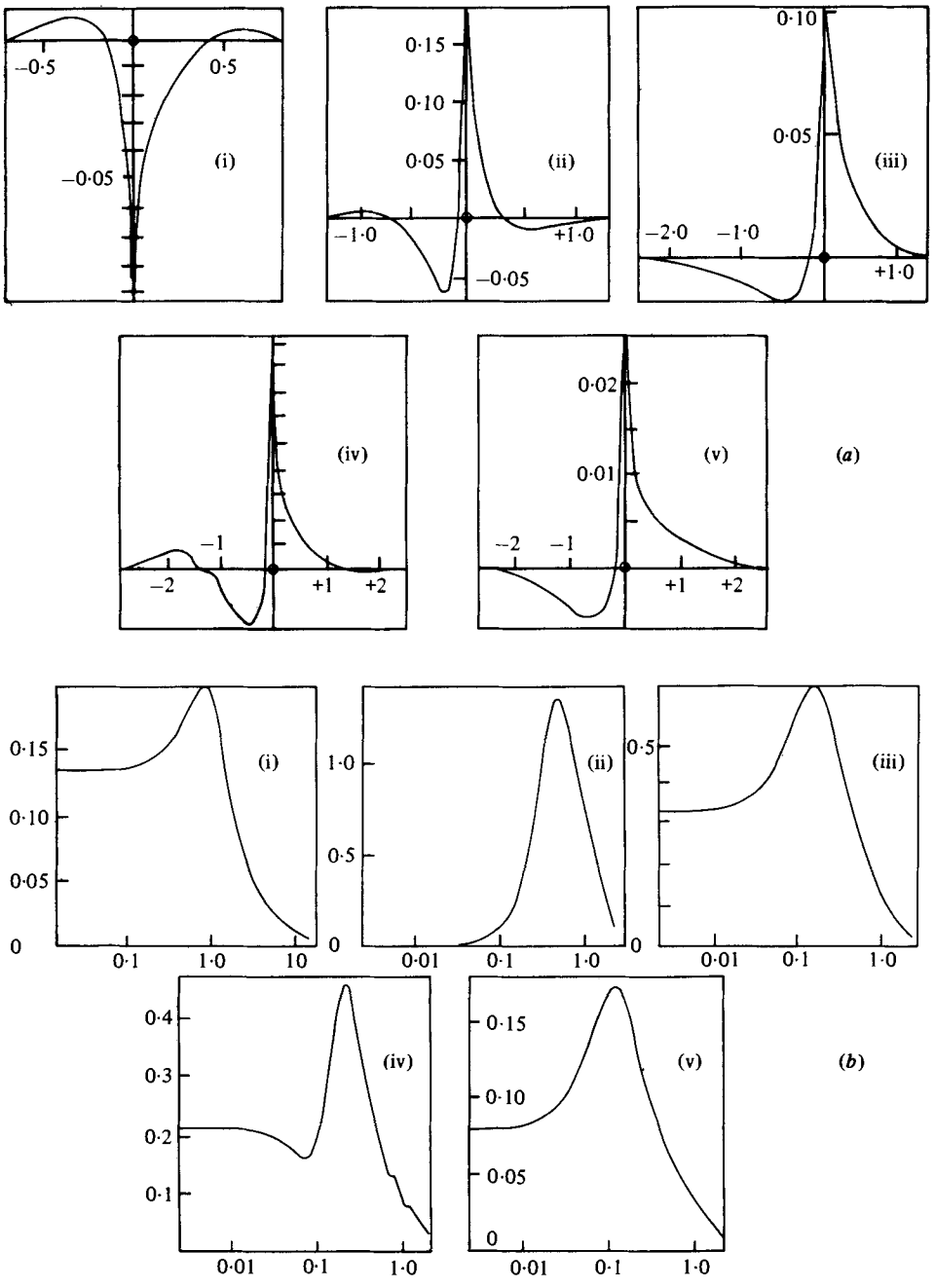

FIGURE 9 (*a*) and (*b*). For legend see facing page.

as it would be expected that the lower frequency, larger scale disturbances would be more constrained by the overall flow geometry and thus present a more orderly structure, whilst the smaller scale disturbances would not be subject to such a constraint. Certainly, where organised structures have been observed, they do correspond to the lower Strouhal numbers under discussion here. It may thus be argued that the

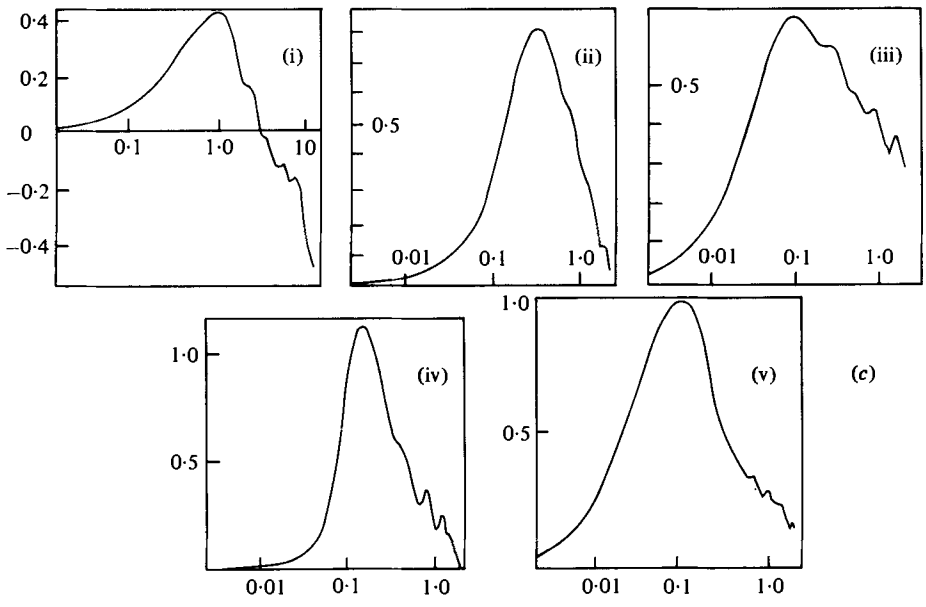

FIGURE 9. Cross correlation of shear and velocity signals. $Re_j = 1{\cdot}77 \times 10^5$. $\Delta y = 0{\cdot}027D$
(*a*) Cross correlations: Vertical scales,

$$\overline{u'(\partial u/\partial y)'}/U_j^2 D;$$

Horizontal scales, $\tau U_j/D$.
(*b*) Co-spectral amplitude: Vertical scales,

$$(1/U_j^2)\,\Phi_{u'(\partial u/\partial y)'}(fD/U_j) \times 10^2;$$

Horizontal scales, fD/U_j.
(*c*) Phase spectra: Vertical scales, radians, shear leading velocity; Horizontal scales, fD/U_j.
(i) $x/D = 1{\cdot}5$, $\eta = -0{\cdot}09$; (ii) $x/D = 1{\cdot}5$, $\eta = +0{\cdot}015$; (iii) $x/D = 1{\cdot}5$, $\eta = 0{\cdot}084$; (iv) $x/D = 6$, $\eta = +0{\cdot}015$; (v) $x/D = 6$, $\eta = 0{\cdot}087$.

vorticity associated with the lower Strouhal number components could well be concentrated more into that component at right angles to both mean flow direction and gradient of mean velocity, one term of which $(\partial u/\partial y)'$ is measured here. Thus the increased relative level of the shear spectrum at low frequencies may be ascribed to the concentration of the turbulent vorticity into a particular component on the larger scales, and the measurement of part of this component by the parallel wire sensor.

Cross correlation of the fluctuating shear signal $(\partial u/\partial y)'$ with the velocity fluctuations indicated by one of the pair of parallel wires (u') give evidence of a distinct phase relation between the two signals. Figure 9(*a*) shows some typical cross correlations measured at $x/D = 1{\cdot}5$ and 6·0. In the results at $x/D = 1{\cdot}5$, the velocity signal used is u_2' at the inner edge of the layer, and u_1' at the outer edge, u_2' being the fluctuation indicated by the wire at the outer radial position in the pair of parallel wires and u_1' the fluctuation indicated by the wire at the inner position. In figure 9(*a*), therefore, the wire which lies more deeply embedded into the turbulent shear layer has been used to indicate the velocity fluctuations. Figures 9(*b*) and (*c*) show the amplitude and phase co-spectra obtained after Fourier transformation of the results of figure 9(*a*) using a digital procedure. The amplitude co-spectra show a strong peak in all cases, this

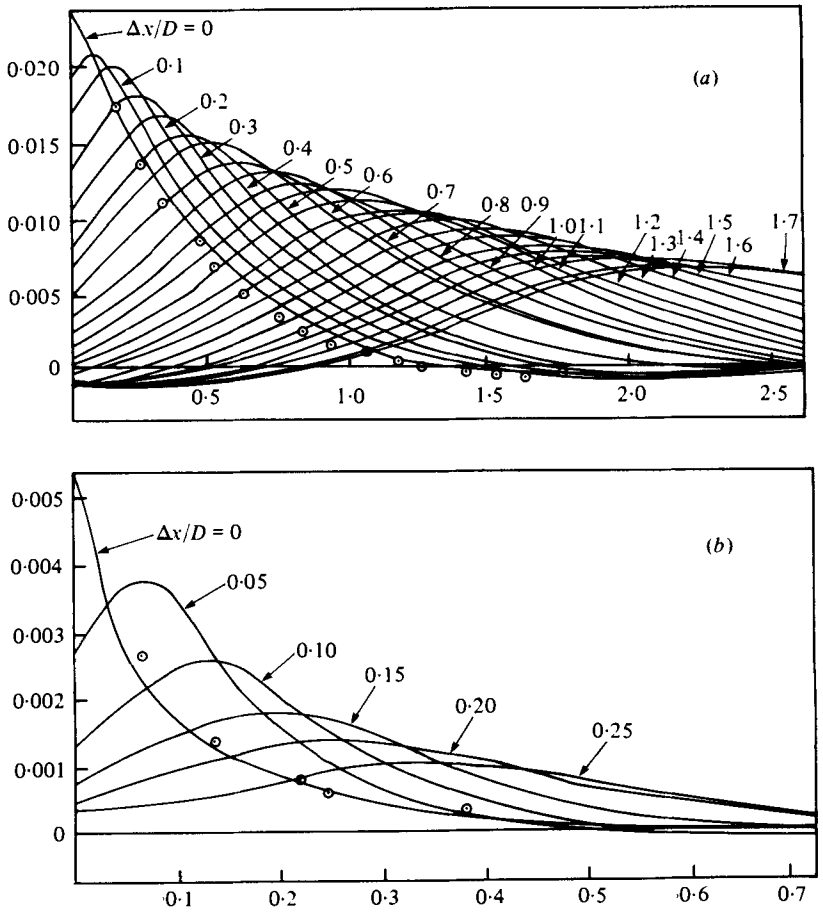

FIGURE 10 (*a*) and (*b*). For legend see facing page.

occurring at lower Strouhal numbers on the outer edge of the shear layer and at positions further downstream where mean local velocities are lower. The phase spectra show that the strongest components exhibit a consistent phase difference between the velocity and shear fluctuations, the shear fluctuations leading the velocity fluctuations by approximately 0·7 radians at $x/D = 1{\cdot}5$ and by slightly over one radian at $x/D = 6$. At very low and high frequencies the phase differences are much smaller, except when the outer radial wire was used to sense velocity at the inside edge of the shear layer at $x/D = 6$. Here the phase reversed at high frequencies as a result of the use of the wire located in the lower mean velocity position to sense velocity.

The presence of a phase lag between two velocity sensors was shown by Browand & Wiedman (1976) to provide evidence for a vortex pairing mechanism within a shear layer, a lag of approximately one radian being an indication that two vortex elements were approaching each other closely. The phase lag observed in the present work can also be viewed as a feature of a structure involving discrete concentrations of vorticity which entrain fluid behich themselves owing to the sense of their rotation. Thus a strong part of the velocity field associated with each concentration of vorticity would pass over the sensor somewhat after the element of vorticity, this corresponding

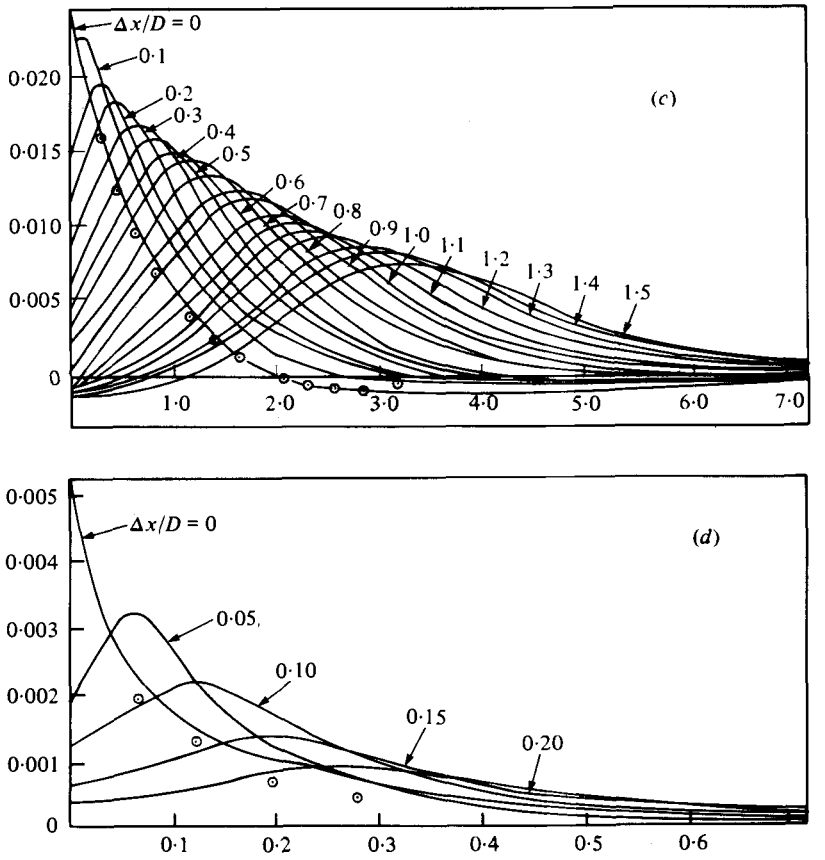

FIGURE 10. Space-time correlations. $Re_j = 1{\cdot}77 \times 10^5$, $\Delta y = 0{\cdot}027D$. Horizontal scales: $\tau U_j/D$. (*a*) $R_{uu}(\tau U_j/D)$, $x/D = 3$, $\eta = 0{\cdot}016$. (*b*) $R_{(\partial u/\partial y)(\partial u/\partial y)}(\tau U_j/D)$, $x/D = 3$, $\eta = 0{\cdot}016$. (*c*) $R_{uu}(\tau U_j/D)$, $x/D = 6$, $\eta = 0{\cdot}016$. (*d*) $R_{(\partial u/\partial y)(\partial u/\partial y)}(\tau U_j/D)$, $x/D = 6$, $\eta = 0{\cdot}016$, ○, $R(\Delta x U_j/U_c D, 0)$.

in general terms to the observations shown in figure 9(*c*). The modest phase lag present is consistent with this argument, as the entrainment behind the vortex element would take place on a physical scale less than the spacing of such elements and so the phase lag detected would not be expected to approach values as large as π for example. The results of figure 9(*c*) show a maximum lag of the order of $\frac{1}{3}\pi$ for the most strongly correlated components.

4. Convection of shear disturbances

Space–time cross correlation measurements for the shear fluctuations were made using two pairs of parallel wires, the front pair being held fixed and the second pair traversed in a streamwise direction behind the first pair. Some results are shown in figure 10(*a*), and it is apparent that the familiar pattern of convection and decay is observed. However, the decay of the shear fluctuations is much faster than that of velocity fluctuations, results at the same position for the latter being shown in figure 10(*b*). Similar measurements were made at a number of positions in the jet over the region $x/D < 6$ and the time for the moving frame autocorrelation to decay to 0·5 for

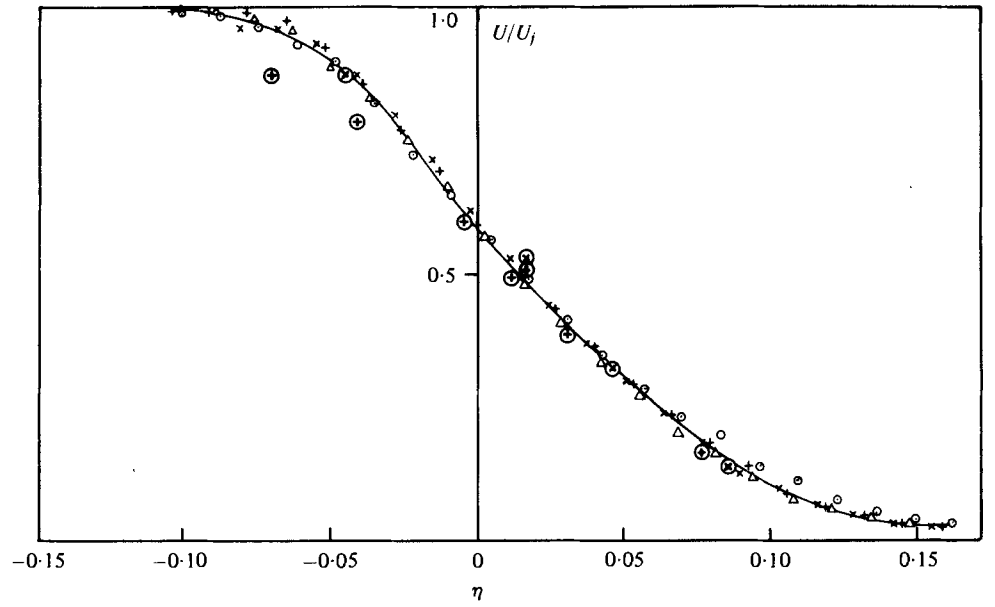

FIGURE 11. Transverse distribution of velocities. $Re_j = 1{\cdot}77 \times 10^5$. Mean velocity: ○, $x/D = 1{\cdot}5$; +, $x/D = 3$; △, $x/D = 4{\cdot}5$; ×, $x/D = 6$. Convection velocity for shear fluctuations: ⊕, $x/D = 3$; ⊗, $x/D = 6$.

these is shown in table 3. The velocity results at equivalent η positions show approximately the expected doubling between $x/D = 3$ and $x/D = 6$, reflecting directly the increase of scale in the velocity structure. However, the decay in terms of the unsteady shear does not show the same effect at all, but remains almost constant between the two axial positions. Whilst it is not possible to draw precise conclusions on the basis of these limited results, it does appear that the turbulent structure when viewed in terms of the fluctuating shear does not show the similar linear growth which appears when viewed in terms of the velocity fluctuations. This lends further support to the conclusion reached earlier on the basis of the intensity of the shear fluctuations that simple scaling of the fluctuations in a given flow on the basis of linear growth of scale in the shear layer does not provide a good description of the observed shear fluctuations.

Figure 10 also shows that the observations of shear and velocity fluctuations both conform to the passage of a convecting decaying structure. The circled points on the space–time correlation denoting $R(\Delta x/U_c, 0)$ may be compared with the autocorrelation $R(0, \tau)$ to demonstrate this. The convection velocity (U_c) of the fluctuations for a number of similar observations of shear fluctuations is shown in figure 11, and it is apparent that it follows the local mean velocity profile much more closely than earlier observations of convection velocity based on velocity fluctuation signals (e.g. Davies *et al.* 1963). In the latter case it has been generally observed that for fluctuations to either side of the centre of the shear layer the convection velocity appeared to lie between the local mean velocity and the mean velocity at the centre of the shear layer, this much smaller variation of convection velocity compared with mean velocity being attributed to the induced velocity effects of the strongest disturbances at the shear layer centre. The present results reflect the fact that the fluctuating shear is essentially

x/D	η	$\left[\frac{\tau_{0.4}U_j}{D}\right]_{\text{vel.}}$	$\left[\frac{\tau_{0.4}U_j}{D}\right]_{\text{shear}}$
3·0	−0·071	1·75	0·38
	−0·043	—	0·15
	−0·005	—	0·14
	+0·016	0·72	0·15*
	+0·016	0·94	0·15
	+0·030	—	0·17
	+0·079	—	0·17
	+0·100	1·52	0·26
6·0	−0·047	1·63	0·11
	+0·013	1·80	0·12*
	+0·016	2·15	0·15
	+0·089	3·41	0·37

TABLE 3. Time for moving frame autocorrelations to decay to 0·4 (all results for $Re_j = 1{\cdot}77 \times 10^5$, except those marked * which apply for $Re_j = 0{\cdot}81 \times 10^5$).

a local effect not influenced in this way by disturbances at a distance from the point of observation, and thus convection and mean local velocities are quite similar in value. It should be noted that these convection velocities have been determined on the basis of tangency to the envelope to the decaying space–time correlations of figure 10, corresponding to the moving frame autocorrelation. Bearing in mind that the correlation at zero separation represents a single shear signal autocorrelation, which relates directly to the spectra which have been discussed earlier, it is seen that the much faster decay of the shear fluctuations compared with the velocity fluctuations (as shown in table 3) is a direct result of the convection of fluctuations in the velocity gradient.

5. Conclusions

The nozzle used in these experiments gave rise to a laminar boundary layer at exit which determined the maximum shear and thickness of the initial laminar shear layer. The flow was not tripped or stimulated in any way, but initially regular disturbances were observed and were confined entirely within the shear layer. Discrete reductions in the frequency of disturbances were observed with increasing distance from the nozzle rather than a progressive reduction of frequency, suggesting that some type of pairing process was occurring. These relatively regular disturbances were confined within the shear layer rather than being a distortion of the complete sheet of vorticity. The disturbances convected at $0{\cdot}59U_j$ and were found to have relatively large peripheral scales. Beyond the point where the second pairing of disturbances occurred the fluctuations extended completely across the shear layer, increasing its growth rate to that of a fully turbulent layer and no longer exhibiting any distinct regularity.

Observations of shear fluctuations in the subsequent fully turbulent shear layer were not found to conform to a pattern of similar growth as the layer thickened. The intensity of the fluctuations reduced more slowly with x than did the mean shear, and correlation measurements showed that the scales were not increasing in proportion to distance from the nozzle. The intensity was found to reduce more nearly with the

half power of distance from an effective origin of the laminar shear layer determined on the basis of the observed shear gradient established by the nozzle exit boundary layer.

It thus appears that viscous diffusion plays a strong role in the scaling of unsteady shear and that the turbulent shear layer is made up of highly convoluted sheets of vorticity. Spectra of the shear fluctuations showed the presence of more energy at lower frequencies in relation to velocity fluctuations than would be expected for homogeneous vorticity, suggesting that lower frequency disturbances contributed more strongly to the component $(\partial u/\partial y)$ observed. This is consistent with a greater directional preference of the shear fluctuations in larger scale disturbances where the influence of the mean velocity field would be stronger and would give rise to increased emphasis of the component aligned with the mean shear which was observed in the present measurements.

The skewness of shear fluctuations remained positive across the entire shear layer indicating that the direction of rotation did not alter as would be expected. Fairly high values of the flatness factor across the whole shear layer, and especially at the inside edge of the shear layer, showed the concentration of shear disturbances into patches of rotation. The shear fluctuations showed a phase lead in relation to velocity disturbances, suggestive of a strong entrainment velocity field behind regions of concentrated rotation. A convecting behaviour was observed in the shear fluctuations and it was found that the apparent convection velocities of the shear fluctuations followed the mean velocity profile more closely than do convection velocities based on velocity fluctuations. It is thus seen than the shear fluctuations represent concentrated and localised disturbances in the turbulent field.

The support of the Science Research Council is gratefully acknowledged.

REFERENCES

BERGER, S. A. 1971 *Laminar Wakes*. New York: Elsevier.

BROWAND, F. K. & WEIDMAN, P. D. 1976 Large scales in the developing mixing layer. *J. Fluid Mech.* **76**, 127–144.

CLEMENTS, R. R. & MAULL, D. J. 1975 The representation of sheets of vorticity by discrete vortices. *Prog. Aero. Sci.* **16**, 129–146.

CORRSIN, S. & KISTLER, A. L. 1955 Free stream boundaries of turbulent flow. *N.A.C.A., Washington. Rep.* no. 1244.

CROW, S. & CHAMPAGNE, F. H. 1971 Orderly structure in jet turbulence. *J. Fluid Mech.* **48** 547–591.

DAVIES, P. O. A. L., BRUUN, H. H. & BAXTER, D. R. J. 1975 Time domain analysis of turbulent structure. *I.S.V.R., Southampton. Memo* no. 529.

DAVIES, P. O. A. L., FISHER, M. J. & BARRETT, M. J. 1963 Turbulence in the mixing region of a round jet. *J. Fluid Mech.* **15**, 337–367.

DAVIES, P. O. A. L. & YULE, A. J. 1975 Coherent structures in turbulence. *J. Fluid Mech.* **71**, 317–338.

DAVIS, M. R. & DAVIES, P. O. A. L. 1972 Factors influencing the heat transfer from cylindrical anemometer probes. *Int. J. Heat Mass Transfer* **15**, 1659–1677.

DAVIS, M. R. 1970 The dynamic response of constant resistance anemometers. *J. Phys.* E **3**(1), 15–20.

DAVIS, M. R. 1971 Measurements in a subsonic turbulent jet using a quantitative Schlieren system. *J. Fluid Mech.* **46**, 631–656.

FIEDLER, H. & HEAD, M. R. 1966 Intermittency measurements in the turbulent boundary layer. *J. Fluid Mech.* **25**, 719–736.

FISHER, M. J. & DAVIES, P. O. A. L. 1964 Correlation patterns in a non-frozen pattern of turbulence. *J. Fluid Mech.* **18**, 97–116.

KISTLER, A. L. 1952 M.S. Thesis. The John Hopkins University.

KOVASZNAY, L. S. G. 1954 Turbulence measurements. *High Speed Aerodynamics and Jet Propulsion*, **19**, 227. Princeton University Press.

KOVASZNAY, L. S. G., KIBENS, V. & BLACKWELDER, R. F. 1970 The intermittent region of a turbulent boundary layer. *J. Fluid Mech.* **41**, 283–325.

KUO, A. Y. S. & CORRSIN, S. 1971 Experiments on internal intermittency and fine structure distribution functions in fully turbulent fluid. *J. Fluid Mech.* **50**, 285–320.

MOORE, C. J. 1977 The role of shear layer instability in jet exhaust noise. *J. Fluid Mech.* **80**, 321–368.

MORRISON, G. L., PERRY, A. E. & SAMUEL, A. E. 1972 Dynamic calibration of inclined and crossed hot wires. *J. Fluid Mech.* **52**, 465–474.

SANDBORN, V. A. 1959 Measurements of intermittency of turbulent motion in a boundary layer. *J. Fluid Mech.* **6**, 221–240.

TOWNSEND, A. A. 1976 *The Structure of Turbulent Shear Flow.* Cambridge University Press.

WINANT, C. D. & BROWAND, F. K. 1974 Vortex pairing: the mechanism of turbulent mixing layer growth at moderate Reynolds number. *J. Fluid Mech.* **36**, 237–255.

WYGNANSKI, I. & FIEDLER, H. E. 1969 Some measurements in the self preserving jet. *J. Fluid Mech.* **38**, 577–612.

WYGNANSKI, I. & FIEDLER, H. E. 1970 The two dimensional mixing region. *J. Fluid Mech.* **41**, 327–361.

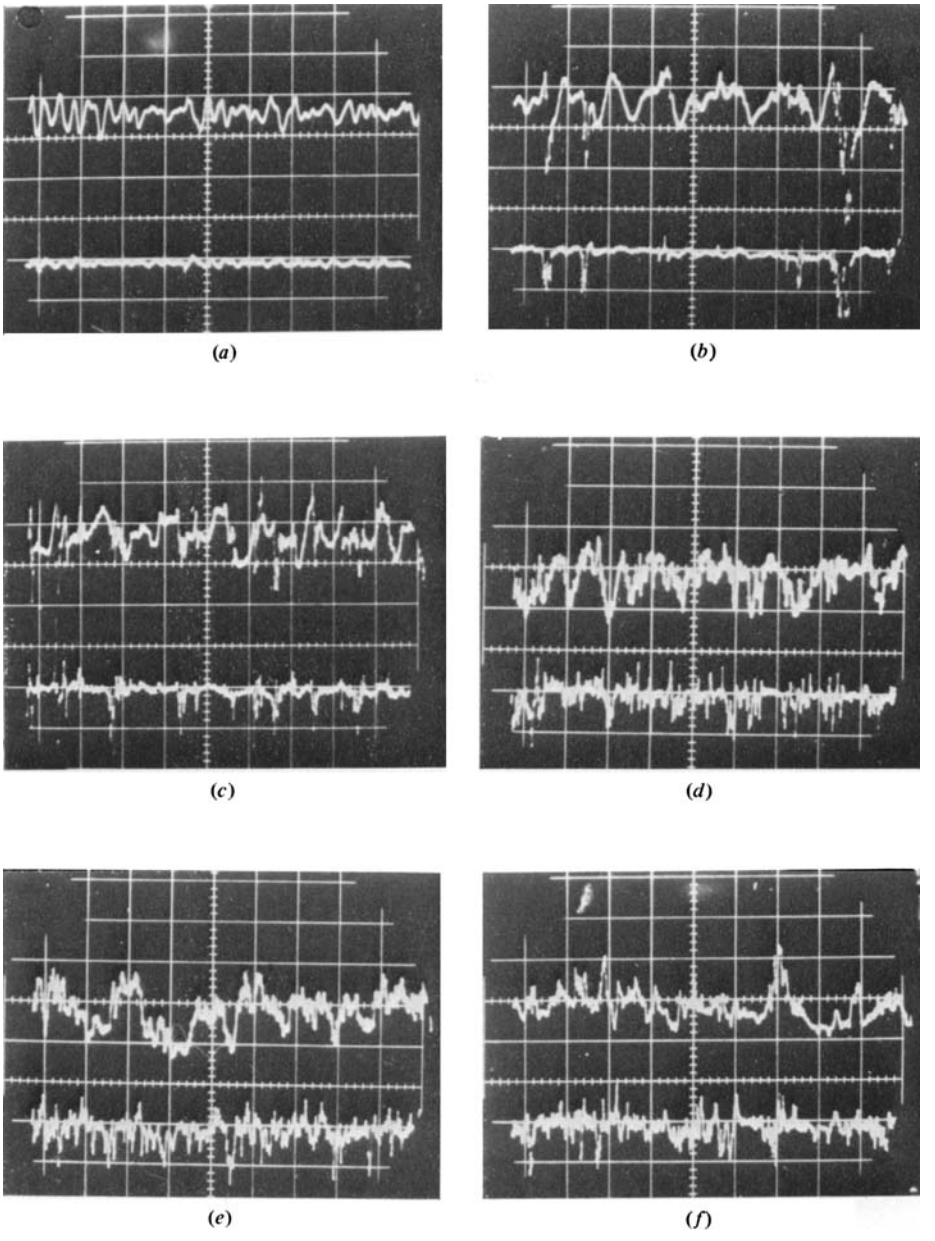

FIGURE 4. Typical wire velocity and velocity difference signals. Upper trace; velocity signal; Lower trace velocity difference ($\Delta y = 0{\cdot}025D$). $Re_j = 1{\cdot}77 \times 10^5$. $x/D = 3{\cdot}0$.

(*a*) Jet axis: 5 ms/cm horizontal; 7·6 m/s/cm vertical (upper); 1·5 m/s/cm vertical (lower). (*b*) $\eta = -0{\cdot}075$, 2 ms/cm horizontal, 7·6 m/s/cm vertical. (*c*) $\eta = -0{\cdot}063$, 2 ms/cm horizontal, 7·6 m/s/cm vertical. (*d*) $\eta = -0{\cdot}040$, 2 ms/cm horizontal, 15·2 m/s/cm vertical. (*e*) $\eta = +0{\cdot}012$, 2 ms/cm horizontal, 15·2 m/s/cm vertical. (*f*) $\eta = +0{\cdot}074$, 2 ms/cm horizontal, 15·2 m/s/cm vertical.